PERGAMON

International Journal of Heat and Mass Transfer 41 (1998) 3841–3856

International Journal of HEAT and MASS TRANSFER

Heat transfer mechanism for Newtonian and non-Newtonian fluids in 2 : 1 rectangular ducts

P. Y. Chang, F. C. Chou*, C. W. Tung

Department of Mechanical Engineering, National Central University, Chung-Li, 320 Taiwan, Republic of China

Received 12 May 1997; in final form 23 February 1998

Abstract

A numerical study has been performed on the heat transfer mechanism of Newtonian and non-Newtonian fluids in 2 : 1 horizontal rectangular ducts. The effects of temperature dependence of viscosity, shear thinning, and buoyancy-induced secondary flow are all considered. Experimental data for Newtonian fluid, water, and non-Newtonian fluid, Separan AP-273 solution (0.1%), were chosen for the comparison with the numerical results. For water, the present numerical results are all in good agreement with the experimental data. The heat transfer enhancement is caused by the buoyancy-induced secondary flow. For Separan AP-273 solution (0.1%), the present numerical results agree with the experimental data in the region near the entrance, but the present modeling underestimates the value of *Nu* in the fully-developed region. In the region near the entrance, the heat transfer enhancement is caused mainly by the axial velocity distortion, which is mainly due to the temperature dependence of viscosity. The effect of buoyancy-induced secondary flow are much weaker in the case for Separan solution rather than that for water. It is mainly caused by the relatively high viscosity of fluid around the central zone of rectangular duct.

Nomenclature

A cross-sectional area of a duct
b viscosity variation parameter defined by equation (1)
C a constant
Cu Carreau number, $\bar{\lambda}\bar{w}/D_h$
D_h hydraulic diameter, $4A/S$
g acceleration due to gravity
Gr_q Grashof number based on constant heat flux, $g\beta\theta_c D_h^3/\bar{\nu}_\infty^2$
Gz Graetz number $(Z/Pr\,Re\,D_h)^{-1}$
h heat transfer coefficient
k thermal conductivity
M, N number of division in X, Y direction, respectively
n power-law index
Nu_l local Nusselt number
P pressure
Pe Peclet number, $Re\,Pr$
Pr Prandtl number, $\bar{\nu}_\infty/\alpha$
Pr_a Prandtl number defined by Xie et al. [2], $\bar{\nu}_a/\alpha$
Pr^* Prandtl number defined by Hartnett et al. [3], Pe/Re^*
q_w uniform heat flux
Q dimensionless parameter for a measure of temperature dependence for viscosity, $b(q_w D_h/k)$
Ra Rayleigh number defined by Hartnett et al. [3], $\rho g\beta(T_w-T_b)D_h^3/\bar{\mu}_w\alpha$
Ra_q Rayleigh number based on constant heat flux, $Pr\,Gr_q$
$Ra_{q,0}$ Rayleigh number, $\rho g\beta q_w D_h^4 C_p/k^2\bar{\nu}_0$
$Ra_{q,a}$ Rayleigh number based on constant heat flux defined by Xie et al. [2], $\rho g\beta q_w D_h^4 C_p/k^2\bar{\nu}_a$
Ra_T Rayleigh number based on wall temperature defined by equation (17), $\rho g\beta(T_w-T_b)D_h^3/\bar{\mu}_\infty\alpha$
Re Reynolds number, $\bar{W}D_h/\bar{\nu}_\infty$
Re_a Reynolds number defined by Xie et al. [2], $\bar{W}D_h/\bar{\nu}_a$
Re^* Reynolds number defined by Hartnett et al. [3],

$$\rho\bar{W}^{2-n}D_h^n\Big/\left[8^{n-1}\left(\frac{a_1+b_1n}{n}\right)^n K\right]$$

T_b bulk temperature
T_w wall temperature
T_{ref} reference temperature

* Corresponding author.

0017–9310/98 $19.00
PII: S0017–9310(98)00093–3

u, v, w dimensionless quantity for U, V and W, respectively
U, V, W velocity components in X, Y, Z directions
x, y, z dimensionless rectangular coordinates
X, Y, Z rectangular coordinates.

Greek symbols
α thermal diffusivity
β coefficient of thermal expansion with temperature
γ dimensionless shear rate
$\bar{\gamma}$ dimensional shear rate
θ dimensionless temperature, $(T-T_{ref})/(q_w D_h/k)$
θ_c characteristic temperature, $q_w D_h/k$
$\bar{\lambda}$ characteristic time of the fluid
μ dimensionless dynamic viscosity
$\bar{\mu}$ dynamic viscosity
$\bar{\nu}$ kinematic viscosity
$\bar{\nu}_a$ apparent kinematic viscosity defined by Xie et al. [2]
ξ vorticity in the axial direction, $\partial u/\partial y - \partial v/\partial x$
ρ density.

Subscripts
ref reference state
w value at the wall
0 very small (zero) shear rate state
∞ very large (infinite) shear rate state.

Superscript
$-$ average value or dimensional state.

1. Introduction

High heat transfer enhancement is required in the design of modern compact heat exchangers and liquid cooling for electronic modules. Recently, significant heat transfer enhancements were reported by Hartnett and his coworkers [1–3] for viscoelastic fluids in a 2 : 1 rectangular channel. The measured heat transfer rates were higher (up to 300%) than the value for the purely forced convection by a Newtonian fluid. Though the surprising results of heat transfer enhancement were reported, the understanding of the mechanism of heat transfer enhancement for these fluids is still limited, because it might be caused by shear-thinning, temperature dependence of viscosity, buoyancy-induced secondary flow, and secondary flow due to normal stress differences.

There are a number of studies on the internal flow heat transfer in circular tubes for Newtonian fluids [4–10]. But in the past few years, the study of heat transfer and flow characteristics in rectangular channels has become increasing important due to the high heat transfer enhancement, which was not observed in the circular tube flow. Kostic [11] addressed the phenomena of laminar heat transfer enhancement in non-circular duct flow of certain non-Newtonian fluids. Xie and Hartnett [12] reported the heat transfer enhancement data for mineral oil in a 2 : 1 rectangular channel. By the numerical studies of Shin et al. [13] and Chou and Tung [14], the mechanism of heat transfer enhancement for mineral oil in a 2 : 1 rectangular channel has been investigated. They found that for the case of top wall heated, the heat transfer enhancement is caused mainly by the axial velocity distortion due to temperature dependence of viscosity. For the cases of bottom wall heated or both top and bottom walls heated, the axial velocity distortion is the major factor in the region near the entrance, while near the fully-developed region, the heat transfer enhancement is mainly caused by the buoyancy-induced secondary flow.

From the foregoing paper review, it is found that the understanding of the mechanism of heat transfer enhancement for Newtonian fluids, such as mineral oil, is quite well. But for the non-Newtonian fluids, the study on the mechanism of heat transfer enhancement is still inadequate. Gingrich et al. [15] investigated the effect of shear thinning on laminar heat transfer behavior in a rectangular duct. Shin and Cho [16] reported the viscosity data of an aqueous polyacrylamide (Separan) solution. They found that the viscosity is strongly temperature-dependent and shear thinning. Gervang and Larsen [17] consider the 'elastic effects' that a non-Newtonian fluid exhibits in fully developed laminar flow in rectangular channels. Gao and Hartnett [18] investigated numerically the fully-developed forced convective flow of a power law non-Newtonian fluid through rectangular channels. Shin and Cho [19] considered the effects of temperature-dependent viscosity and shear thinning in the entrance region of top-heated rectangular channels. It is worthy to note that they did not include the effect of secondary flow. Gao and Hartnett [20, 21] used a Reiner–Rivlin constitutive equation to study heat transfer behavior of non-Newtonian fluids in the fully-developed region of rectangular ducts. They reported that heat transfer enhancement is caused by secondary flows, which arise from normal stress differences under shearing flow conditions. There is still no thorough study of mechanism of heat transfer enhancement for non-Newtonian fluid, such as Separan solution, in the entrance region of rectangular channels. In the present paper, the effects of temperature-dependent viscosity, shear thinning and buoyancy-induced secondary flow are all considered to model the heat transfer behavior for water and Separan solution in the entrance region of a rectangular channel.

2. Theoretical analysis

Consider a steady three-dimensional laminar flow in the entrance region of a horizontal 2 : 1 rectangular channel as shown in Fig. 1. The channel is adiabatic at the side walls. The heating conditions considered in the present work follows those in Hartnett and Kostic [3] : upper

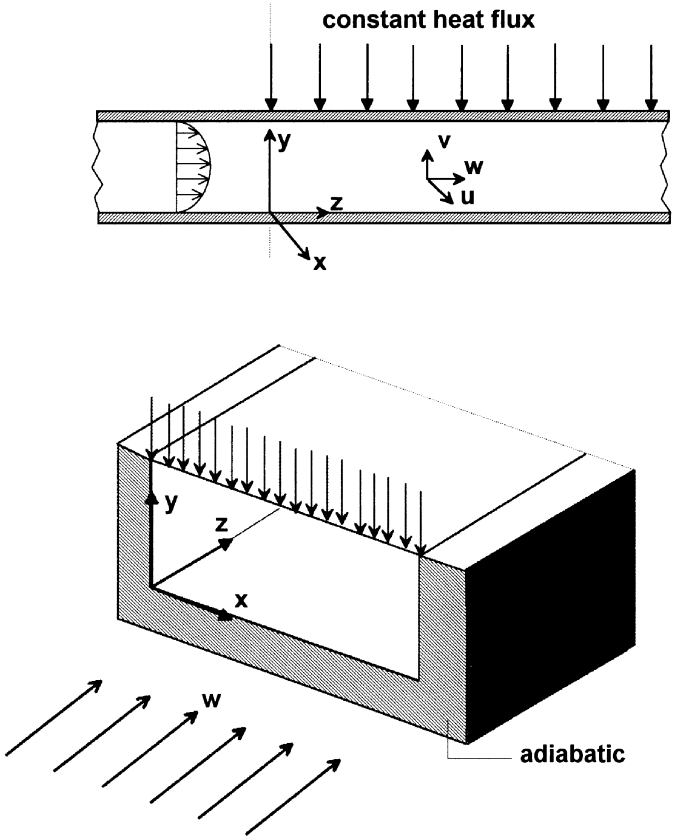

Fig. 1. Physical configuration for upper wall heated condition and the coordinate system.

wall heated, lower wall heated, and both upper and lower walls heated. The viscosity model used in the present computation is adopted after Kwant and Ravenstein [22] who proposed simple power law multiplied by an exponential decay function of temperature. As considered in Chou et al. [23]: to avoid singularity in computation, the power law is replaced by the Carreau model (Bird et al. [24]) which characterize the shear-thinning effect. The final expression become:

$$\bar{\mu} = \exp[-b(T-T_{\mathrm{ref}})]\{\bar{\mu}_\infty + (\bar{\mu}_0 - \bar{\mu}_\infty)[1+(\bar{\lambda}\bar{\gamma})^2]^{(n-1)/2}\} \tag{1}$$

or in dimensionless form:

$$\mu = \frac{\bar{\mu}}{\bar{\mu}_{\mathrm{ref},\infty}} = \exp(-Q\theta)\{\mu_\infty + (\mu_0 - \mu_\infty)[1+(Cu\gamma)^2]^{(n-1)/2}\} \tag{2}$$

where b is a viscosity variation parameter, $\theta = (T-T_{\mathrm{ref}})/\theta_{\mathrm{c}}$ is a dimensionless temperature, $\theta_{\mathrm{c}} = q_{\mathrm{w}}D_{\mathrm{h}}/k$ is a characteristic temperature, $Q = b(q_{\mathrm{w}}D_{\mathrm{h}}/k)$ is a measure of magnitude of temperature dependence for viscosity, and $\bar{\mu}_0$ is the zero-shear-rate viscosity at T_{ref}, $\bar{\mu}_\infty$ is the infinite-shear-rate viscosity at T_{ref}. $\bar{\gamma}$ and γ are dimensional and dimensionless shear rate, respectively. $(n-1)$ is the power-law slope of viscosity with respect to shear rate. $\bar{\lambda}$ is the characteristic time equal to reciprocal of the shear rate at which shear thinning begins, and it is also temperature dependent as reported by Shin and Cho [16]:

$$\bar{\lambda} = \bar{\lambda}_{\mathrm{ref}} 10^{\zeta\theta_{\mathrm{b}}} \tag{3}$$

where $\bar{\lambda}_{\mathrm{ref}}$ represents the value at the reference temperature: 20°C. The exponent ζ is a constant value -14.9 for Separan AP-273 (0.1%) fluid, $\theta_{\mathrm{b}} = (T_{\mathrm{b}}-T_{\mathrm{ref}})/(q_{\mathrm{w}}D_{\mathrm{h}}/k)$, $Cu = \bar{\lambda}\bar{W}/D_{\mathrm{h}}$ is the Carreau number in which $\bar{W}$ is the averaged axial velocity. When the value of Q is zero, equation (2) is reduced to the Carreau model. To summarize the present viscosity model, one observes two factors influencing the viscosity μ. First, the temperature effect on the viscosity is explicitly given in the exponential form. Second, the Carreau model in the equation deals with the shear thinning phenomenon.

2.1. *Governing equations*

The Boussinesq approximation is used to characterize the buoyancy effect. The viscous dissipation and com-

pression effects are neglected. The dimensionless variables are introduced:

$$x=\frac{X}{D_h},\quad y=\frac{Y}{D_h},\quad z=\frac{Z}{Pr\,Re\,D_h},\quad u=\frac{U}{U_0},$$

$$v=\frac{V}{U_0},\quad w=\frac{W}{\bar{W}},\quad \gamma=\frac{\bar{\gamma}D_h}{W}\quad \theta=\frac{T-T_{ref}}{\theta_c},$$

$$p=\frac{P}{\rho\bar{W}\bar{v}_\infty/D_h},\quad v=\frac{\bar{v}}{\bar{v}_\infty},\quad Pr=\frac{\bar{v}_\infty}{\alpha},\quad Re=\frac{\bar{W}D_h}{\bar{v}_\infty},$$

$$Pe=Pr\,Re,\quad Gr_q=\frac{g\beta\theta_c D_h^3}{\bar{v}_\infty^2},\quad Ra_q=Pr\,Gr_q \tag{4}$$

where

$$D_h=\frac{4A}{S},\quad U_0=\frac{Gr_q\bar{v}_\infty}{D_h},\quad \theta_c=\frac{q_w D_h}{k}.$$

By introducing a vorticity function in the axial direction, $\xi=\partial u/\partial y-\partial v/\partial x$, the vorticity–velocity formulation of Navier–Stokes equations can be derived and shown as follows:

$$\nabla^2 u=\frac{\partial\xi}{\partial y}-\frac{1}{Ra_q}\left(\frac{\partial^2 w}{\partial x\,\partial z}\right) \tag{5}$$

$$\nabla^2 v=-\frac{\partial\xi}{\partial x}-\frac{1}{Ra_q}\left(\frac{\partial^2 w}{\partial y\,\partial z}\right) \tag{6}$$

$$\begin{aligned}&Gr_q\left(\xi\frac{\partial u}{\partial x}+\xi\frac{\partial v}{\partial y}+u\frac{\partial\xi}{\partial x}+v\frac{\partial\xi}{\partial y}\right)\\&\quad+\frac{1}{Pr}\left(\frac{\partial w}{\partial y}\frac{\partial u}{\partial z}-\frac{\partial w}{\partial x}\frac{\partial v}{\partial z}+w\frac{\partial\xi}{\partial z}\right)\\&=v\nabla^2\xi+2\left(\frac{\partial v}{\partial y}\right)\nabla^2 u-2\left(\frac{\partial v}{\partial x}\right)\nabla^2 v+2\frac{\partial^2 v}{\partial x\,\partial y}\left(\frac{\partial u}{\partial x}-\frac{\partial v}{\partial y}\right)\\&\quad+\left(\frac{\partial^2 v}{\partial y^2}-\frac{\partial^2 v}{\partial x^2}\right)\left(\frac{\partial v}{\partial x}+\frac{\partial u}{\partial y}\right)-\frac{\partial\theta}{\partial x}\end{aligned} \tag{7}$$

$$\begin{aligned}&Gr_q\left(u\frac{\partial w}{\partial x}+v\frac{\partial w}{\partial y}\right)+\frac{1}{Pr}\left(w\frac{\partial w}{\partial z}\right)\\&=-\frac{1}{Pe}\left(\frac{\partial p}{\partial z}\right)+v\nabla^2 w+\frac{\partial v}{\partial x}\frac{\partial w}{\partial x}+\frac{\partial v}{\partial y}\frac{\partial w}{\partial y}\end{aligned} \tag{8}$$

$$Ra_q\left(u\frac{\partial\theta}{\partial x}+v\frac{\partial\theta}{\partial y}\right)+w\frac{\partial\theta}{\partial z}=\nabla^2\theta \tag{9}$$

where $\nabla^2=(\partial^2/\partial x^2+\partial^2/\partial y^2)$. It should be noted that the axial diffusion terms in equations (7)–(9) are neglected under the condition of high Peclet number.

2.2. *Boundary conditions*

At the entrance $z=0$, the flow is considered as hydrodynamically fully developed. So the axial velocity w must satisfy

$$\nabla^2 w=C \tag{10}$$

where $C=-(1/Pe)(\partial p/\partial z)=$ constant and the constraint: $\bar{w}=1$. Because of symmetry, it suffices to solve the problem in a half region of the rectangular duct. Therefore, the boundary conditions are as follows:

$$\begin{aligned}&u=v=w=0\quad\text{on all walls}\\&\frac{\partial\theta}{\partial n}=1\quad\text{on the heated wall}\\&\frac{\partial\theta}{\partial n}=0\quad\text{on the adiabatic wall}\\&\theta=u=v=\xi=0,\quad \bar{w}=1\quad\text{at the entrance}\\&u=\frac{\partial v}{\partial x}=\frac{\partial w}{\partial x}=\frac{\partial\theta}{\partial x}=\frac{\partial\xi}{\partial x}=0\\&\text{at the plate of symmetry.}\end{aligned} \tag{11}$$

After the developing velocity profile and temperature fields along the axial direction are obtained, the local Nusselt number Nu_1 can be calculated, and the calculation is based on the overall energy balance for axial length dz and the temperature gradient on the heated wall.

$$Nu_1=\frac{\bar{h}D_h}{k_f}=\frac{1}{\overline{w(\bar{\theta}_w-\theta_b)}} \tag{12}$$

where k_f is the thermal conductivity of fluid, $\bar{\theta}_w$ is the averaged wall temperature, and θ_b is the fluid bulk mean temperature. Simpson's rule is used to compute the average quantities indicated above.

Though the governing equations (5)–(9) are more complicated than those shown in Chou and Hwang [25], the computation procedure for the simultaneous solutions of equations (5)–(9) with boundary conditions (10)–(11) is the same in principle.

3. Results and discussion

Numerical experiments were carried out to ensure the accuracy of the present results. First, the values of bulk mean temperature θ_b were checked by the known analytical results $\theta_b=4z/3$ for the cases of upper wall heated or lower wall heated and $\theta_b=8z/3$ for the case of both upper and lower walls heated. The above-mentioned analytical results may be obtained by considering an overall energy balance for a dimensionless axial length dz. The deviations were seen to be less than 1.5%.

A comparison of the present numerical modeling with the existing experimental data (Hartnett and Kostic [3]) is used to study the mechanism of heat transfer enhancement for water and Separan AP-273 solution (0.1%). But only the data of Rayleigh number Ra, Reynolds number Re^*, and Prandtl number Pr^* were shown in Hartnett and Kostic [3]. Therefore, the transformation of the foregoing parameters to the parameters Pr, Ra_q and Q, which are used in the present study, is first required. To obtain the values of $Q = b(q_w D_h/k)$ from the available data, the constant value b must be determined. For water, the temperature dependence of viscosity is $\bar{\nu}_{20^\circ C}/\bar{\nu}_{50^\circ C} = 1.816$. Then we can obtain $b = 0.019$ from equation (1). But for Separan AP-273 solution (0.1%), there is a large variation for the value b in equation (1). It will be discussed later. The following equations are used to calculate $\theta_c (= q_w D_h/k)$.

$$Ra_q = Ra_T \times (Nu_1)_{fd} \tag{13}$$

$$Pr\, Gr_q = (g\beta D_h^3/\alpha^2)(q_w D_h/k) = Ra_{q,a} \tag{14}$$

where $(Nu_1)_{fd}$ is local Nusselt number in the fully developed region. One may ask why we did not calculate θ_c directly from the data of Ra_q or Gr_q. It is worthy to note that the value of $\bar{\nu}_\infty$ in Ra_q or Gr_q in equation (4) is rather temperature sensitive, therefore, it is hard to obtain the corresponding values of θ_c in the experimental work of Hartnett and Kostic [3] directly from the data of Ra_q or Gr_q. But the value of α is relatively temperature insensitive, and θ_c can be obtained from the equation (14).

Figure 2 presents the variation of local Nusselt number Nu_1 vs. z for water with only upper wall heated and others walls adiabatic in a 2:1 rectangular duct. The present modeling shows an excellent agreement with the experimental data of Hartnett and Kostic [3]. Since only upper wall is heated, the effect of buoyancy-induced secondary flow on the value of Nu_1 is rather weak. The variation of Nu_1 vs. z for the case of both upper and lower walls heated is shown in Fig. 3. One can see that Nusselt number variations on the upper and lower heated walls are also shown. On the lower wall, the Nusselt number is at first decreasing to a local minimum, and then gradually increasing due to the buoyancy-induced secondary flow. While on the upper wall, the variation of Nusselt number is rather similar to that shown in Fig. 2. The present modeling again shows an excellent agreement with the experimental data [3]. From the above comparison of the present modeling with the experimental data [3], we may say that the heat transfer enhancement mechanism for water, which is caused by the buoyancy-induced secondary flow, is rather clear now.

Then we try to study the mechanism of heat transfer enhancement for non-Newtonian fluids, such as Separan AP-273 solution (0.1%). The first task is the modeling of viscosity. The second task is the modeling of the axially developing secondary flow, which is induced both by the buoyancy effect and the normal stress differences.

Concerning the modeling of viscosity, the data of viscosity variation for Separan AP-273 solution (0.1%) by Hartnett [1] and Xie and Hartnett [2] are reshown in Fig. 4. The viscosity data from Xie and Hartnett [2] is those for 63 h of circulation. In Fig. 4, one can find that the viscosity is only changed with shear rate, and the data can be well fitted by equation (1). It is worthy to note that the temperature dependence of viscosity for Separan AP-273 solution (0.1%) was not reported by Hartnett [1], Xie and Hartnett [2], and Hartnett and Kostic [3]. Besides, the temperature effect on viscosity over the studied temperature range was considered negligible or like that of water by Kostic [26] and Xie [27]. But Shin and Cho [19] showed that the viscosity depends both on shear-rate and temperature as shown in Fig. 5. They pointed out that one of the possible reasons for this obvious difference is the effect of solvent. Tap water was used as the solvent by Kostic [26] and Xie [27], while distilled water was used by Shin and Cho [19]. We found that the second possible reason might be that the significant temperature dependence of viscosity is seen at the zero-shear-rate range by Shin and Cho [19], but Kostic [26] and Xie [27] did not show the range of shear rate at which they evaluated the effect of temperature on viscosity. It is also noted in Xie [27] that there is a large viscosity variation with the hours of circulation. In the present work, we focused on the effects of shear thinning, temperature dependence of viscosity and buoyancy-induced secondary flow on the laminar heat transfer of Separan AP-273 solution (0.1%). The effect of the axially developing secondary flow, which is induced by the normal stress differences, will be the scope of our future work.

The comparison of the present numerical results of Nusselt number variation with the data of Xie and Hartnett [2] is shown in Fig. 6 for the Separan AP-273 solution (0.1%). It is noted that only upper wall is heated while the other three walls are adiabatic. The present numerical results are obtained by the viscosity modeling, which is corresponding to the data of 63 h of circulation. To transfer the value of parameters in Xie and Hartnett [2] to the present modeling, the following values of viscosity of fluid for 63 h of circulation in Xie and Hartnett [2] are considered: at shear-rate $\bar{\gamma} = 0.5$ (1/s), the viscosity $\bar{\mu}_0 = 17.56$ cp (centipoise); at shear-rate $\bar{\gamma} = 500$ (1/s), the viscosity $\bar{\mu}_\infty = 5.65$ cp, and this value is also the reference value $\bar{\mu}_{\infty,ref}$ in the present modeling. The values of Prandtl number Pr and Rayleigh number Ra_q will be calculated by this value. It should be noted that the parameters set: $Ra_q = 9.35 \times 10^5$ and $Pr = 37.1$ in this numerical work shown in Fig. 6 is corresponding to the set: $Ra_{q,a} = 4.83 \times 10^5$, and $Pr_a = 71.8$ in the experimental work of Xie and Hartnett [27]. The characteristic time $\bar{\lambda}_{ref} = 0.1$ (s), $\bar{w} = 0.122$ (m s^{-1}), and $D_h = 0.012$ (m), so the initial Carreau number $Cu_i = \bar{\lambda}\bar{w}/D_h = 1.0167$. As

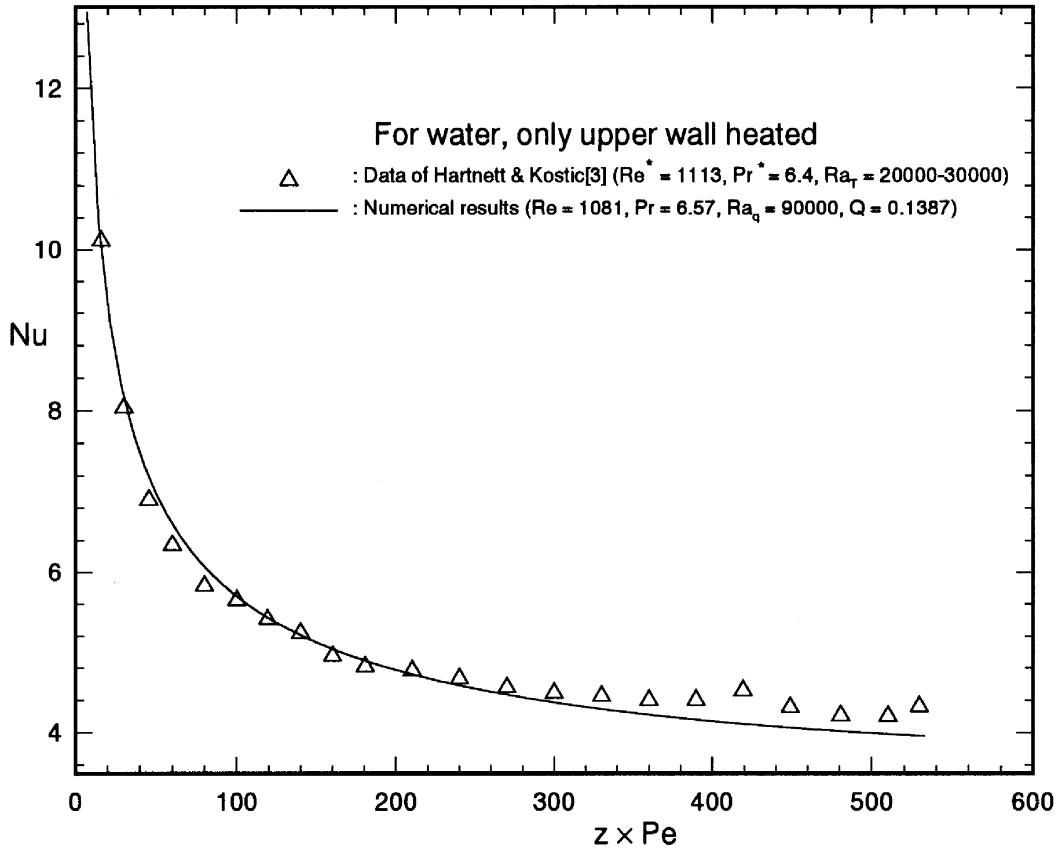

Fig. 2. The comparison of the present numerical results of Nu with experimental data for water under the heating condition of only upper wall heated.

already shown in Fig. 4, the viscosity change is rather small for the fluid of 63 h of circulation. So $b = 0.019$, which is usually used for water, is used here as considered by Xie [27]. From equation (18), the value of $q_w D_h/k$ can be calculated from the experimental data, and then $Q = b(q_w D_h/k)$ about 5.0 is obtained. To demonstrate whether there is heat transfer enhancement or not, the curve of Nu for purely forced convection ($Ra_q = 0$ and $Q = 0$) is also shown in Fig. 6 for comparison. It is seen that the curve of $Ra_q = 9.35 \times 10^5$, $Pr = 37.1$ and $Q = 5.0$ falls above the curve of purely forced convection for $Gz < 10^4$ due to the heat transfer enhancement, and the curve of $Ra_q = 9.35 \times 10^5$, $Pr = 37.1$ and $Q = 5.0$ shows a better agreement with the data of $Ra_{q,a} = 4.83 \times 10^5$ and $Pr_a = 71.8$ especially in the region near the entrance ($Gz > 50$). Compared with the experimental data, the present modeling still underestimates the value of Nu in the fully-developed region. This underestimation is believed to be caused by the exclusion of the secondary flow induced by the normal stress differences as reported by Gao and Hartnett [21] in the present numerical modeling. To study the mechanism of heat transfer enhancement, the axial development of velocity distributions $w = W/\bar{W}$ along y at the symmetry plane ($x = 0.75$) are shown in Fig. 7. It is seen that the velocity distribution is quite symmetric at $Gz = 3 \times 10^3$. But as Gz decreases, the velocity distributions are more and more distorted toward the heated upper wall. By a comparison of Figs 6 and 7, one can find that with stronger velocity distortion at $Gz = 50$, there is a stronger heat transfer enhancement at $Gz = 50$. This axial velocity distortion is mainly due to the temperature dependence of viscosity. The distortion of axial velocity will induce secondary flow. The secondary flows at $Gz = 3 \times 10^3$ and 50 are shown in Fig. 8(a)–(b). The motions of secondary flow are mainly upward at $Gz = 3 \times 10^3$ especially in the central zone of Fig. 8(a). But it is seen in Fig. 8(b) that there are both upward and downward motions for secondary flow at $Gz = 50$, and a clockwise vortex is formed. But the magnitude of downward motion is smaller than that of upward motion. This kind of secondary flow pattern is caused by the combined effects of axial velocity distortion and buoyancy-induced secondary flow. The value of $Ra_q = 9.35 \times 10^5$ is not small but it should be noted that

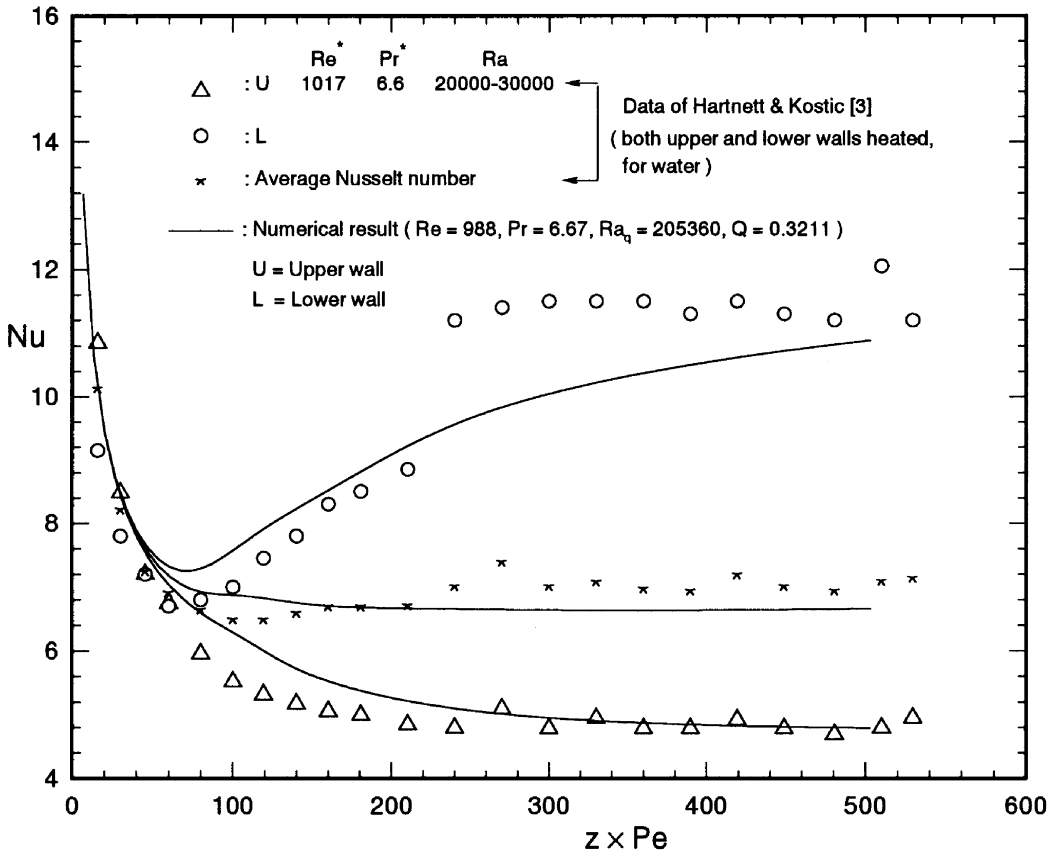

Fig. 3. The comparison of the present numerical results of *Nu* with experimental data for water under the heating condition of both upper and lower walls heated.

the value of Ra_q is evaluated by $\bar{\nu}_\infty$. In other words, the actual buoyancy effect in this upper wall heated case is smaller if the value of Ra_q is evaluated by $\bar{\nu}_0$, the viscosity around the central zone of rectangular channel. The corresponding value is $Ra_{q,0} = 3 \times 10^5$.

Another heat transfer performance of the Separan AP-273 solution (0.1%) is shown in Fig. 9 for the case that both the upper and lower walls are heated while the other two walls are adiabatic. Hartnett and Kostic's experimental data [3] is used for comparison with the numerical results. From the Hartnett's viscosity data [1], which is already shown in Fig. 4, one can obtain that: at shear-rate $\bar{\gamma} = 0.001$ (1 s^{-1}), the viscosity $\bar{\mu}_0 = 216$ cp; at shear-rate $\bar{\gamma} = 23\,991$ (1/sec), the viscosity $\bar{\mu}_\infty = \bar{\mu}_{\infty,\mathrm{ref}} = 3.099$ cp; the characteristic time $\bar{\lambda}_{\mathrm{ref}} = 3.02$ (s). For different flow velocities $\bar{w} = 0.85$ and 1.1 (m s^{-1}), the initial Carreau numbers are $Cu_i = 214$ and 277, respectively. Because the viscosity change is very large, $b = 0.1$ was considered as shown in Shin and Cho [16] for this simulation, then $Q = 19$ and 19.4, respectively. At the region of high Graetz number (near the entrance), the numerical results are in good agreement with experimental data. But the present modeling again underestimates the value of *Nu* in the fully-developed region. To study the mechanism of heat transfer enhancement, the axial development of velocity distributions $w = W/\bar{W}$ along y at the symmetry plane ($x = 0.75$) are shown in Fig. 10. It is seen that the velocity distributions are always symmetric. But as Gz decreases, the velocity distributions are more and more flat. The velocity distributions are symmetrically distorted toward the heated upper and lower walls. By a comparison of Fig. 9 and 10, one can find that with stronger velocity distortion at $Gz = 200$ than that at $Gz = 3 \times 10^3$, there is a stronger heat transfer enhancement at $Gz = 200$. This axial velocity distortion is mainly due to the temperature dependence of viscosity. The distortion of axial velocity will induce secondary flow. The secondary flows at $Gz = 3 \times 10^3$ and 200 are shown in Fig. 11(a)–(b). The motions of secondary flows are almost symmetric with respect to $y = 0.375$ at $Gz = 3 \times 10^3$ in Fig. 11(a). But it is seen in Fig. 11(b) that the secondary flow pattern is no more symmetric, and it can be considered as a superposition of secondary flows which are induced by the axial velocity distortion and buoyancy

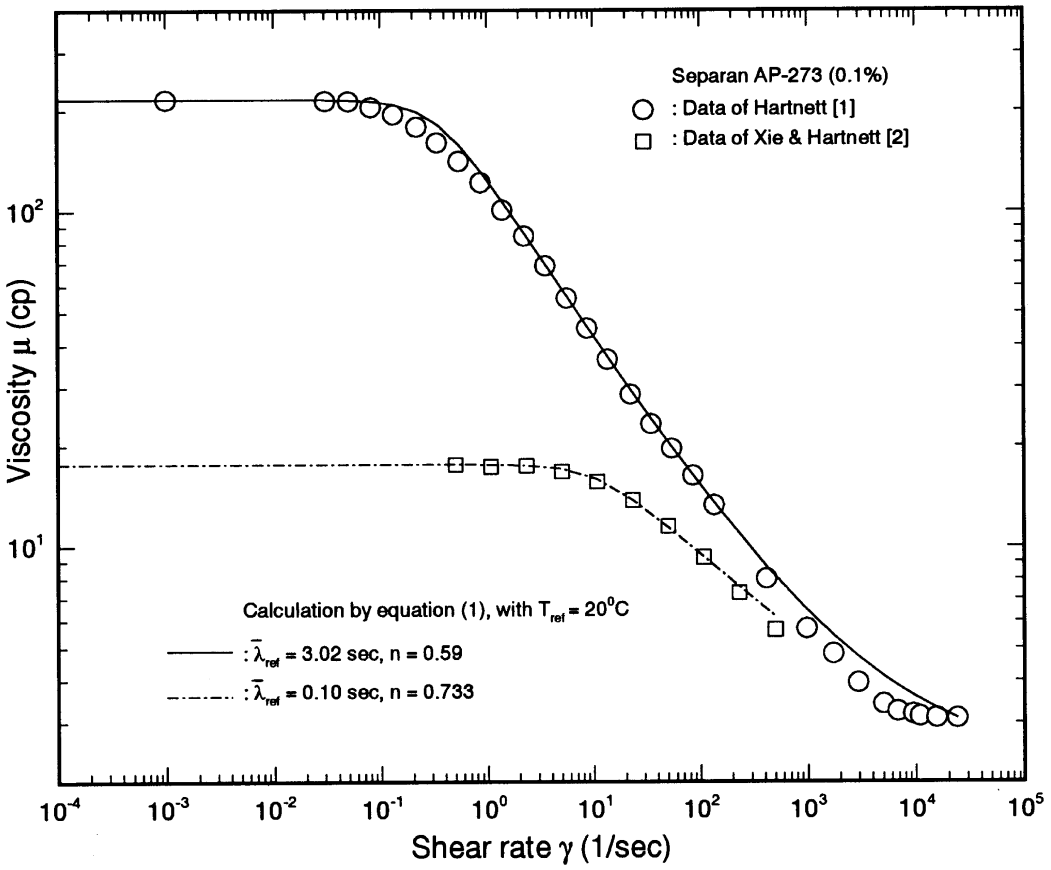

Fig. 4. Numerical modeling and experimental data of the shear thinning viscosity for Separan AP-273 solution (0.1%).

effect, respectively. By a deeper inspection of the magnitude of secondary flows in Fig. 11(a) and (b), one can see that the strength of secondary flow in Fig. 11(a) is almost ten times larger than that in Fig. 11(b). In other words, the buoyancy-induced secondary flow is rather weak. The value of $Ra_q = 1.33 \times 10^6$ is not a small value. But if Ra_q is evaluated by $\bar{v}_0$, the viscosity around the central zone of rectangular channel, the corresponding $Ra_{q,0} = 1.93 \times 10^4$ is even one order smaller than that in Fig. 6.

From the present modeling, we found that the heat transfer enhancement for Separan AP-273 solution (0.1%) in the region near the entrance is caused by the axial velocity distortion. And the axial velocity distortion is mainly caused by the temperature dependence of viscosity. But in the fully-developed region, the present modeling underestimated the value of Nusselt number. It is believed that the secondary flows caused by the normal stress differences may be the reason for the heat transfer enhancement in the fully-developed region as reported by Gao and Hartnett [21].

4. Concluding remarks

A numerical study has been done to investigate the laminar flow and heat transfer behaviors of Newtonian and non-Newtonian fluids in a 2 : 1 horizontal rectangular duct. The effects of temperature dependence of viscosity, shear thinning, and buoyancy-induced secondary flow are all considered to model the laminar flow and heat transfer behaviors. Experimental data for Newtonian fluid, water, and non-Newtonian fluid, Separan AP-273 solution (0.1%), were chosen for the comparison with the numerical results. For water, the present numerical results are all in good agreement with the experimental data of Hartnett and Kostic [3]. For Separan AP-273 (0.1%), the present numerical results agree with the data [2, 3] in the region near the entrance, but the present modeling underestimates the value of Nu in the fully-developed region. The key findings are as follows:

(1) For Newtonian fluid, water, Nusselt number decreases along the axial direction and finally reach

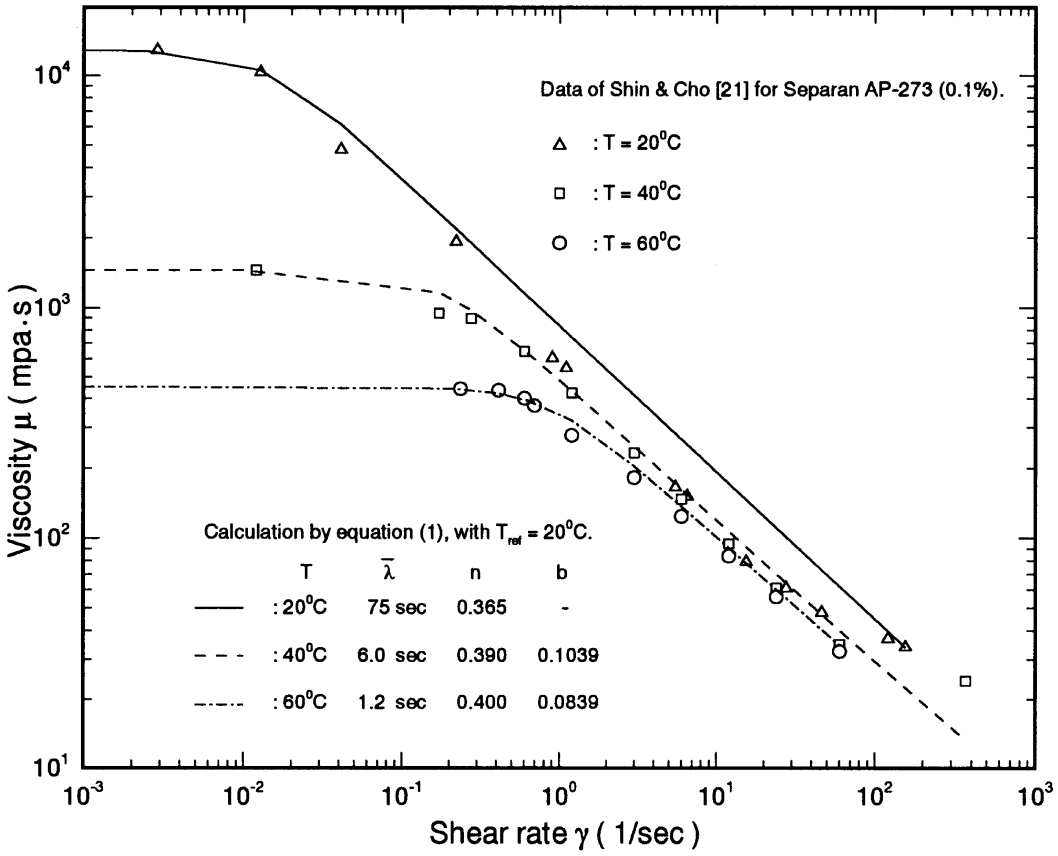

Fig. 5. Numerical modeling and experimental data of the shear thinning and temperature-dependent viscosity for Separan AP-273 solution (0.1%).

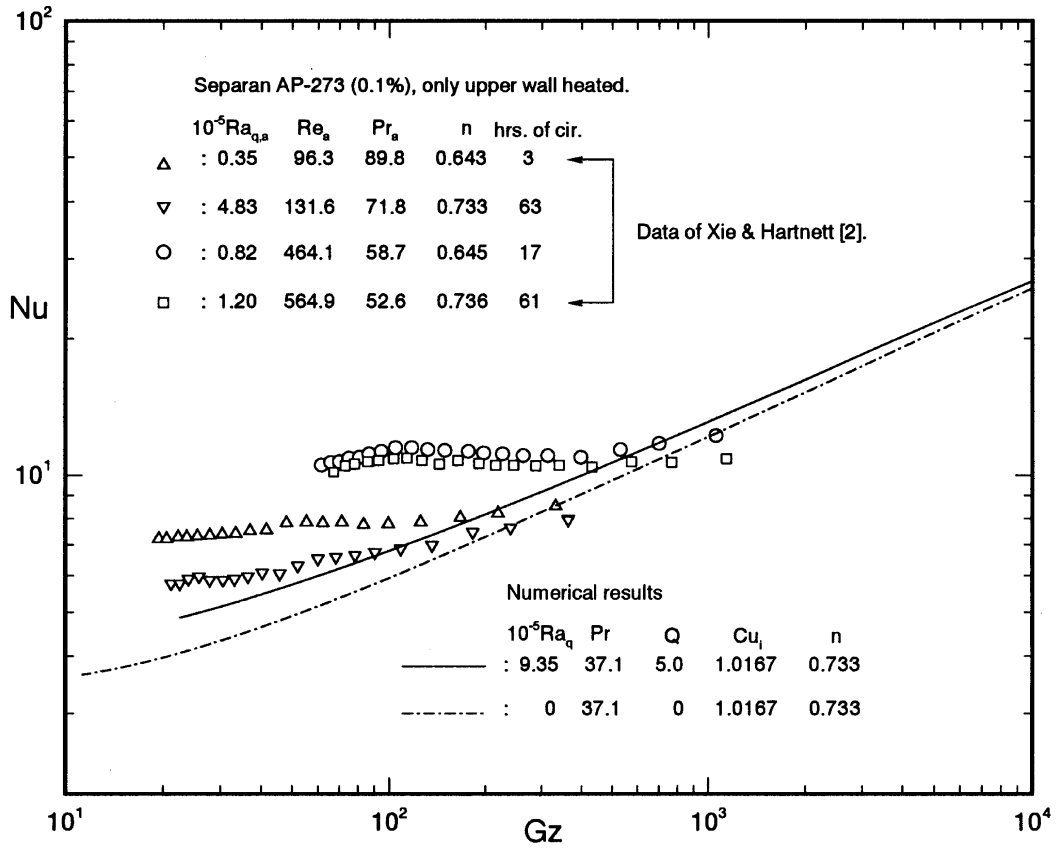

Fig. 6. The comparison of the present numerical results of *Nu* with experimental data for Separan solution under the heating condition of only upper wall heated.

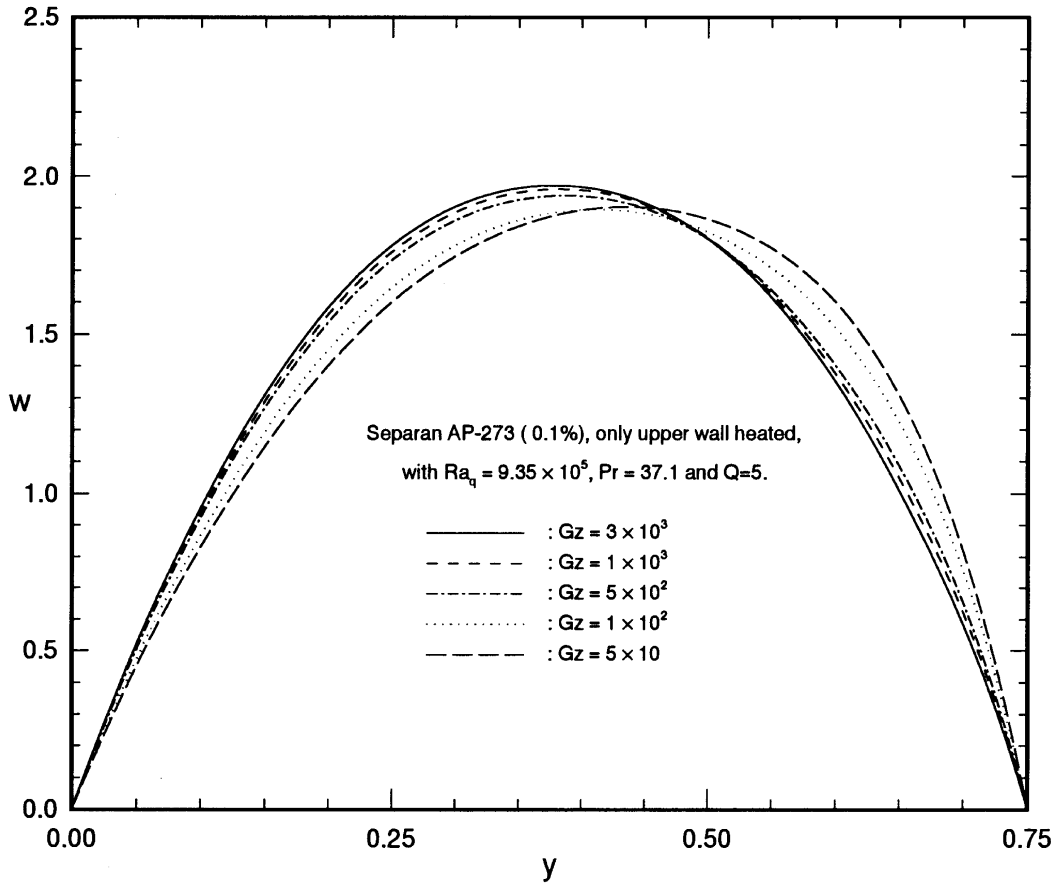

Fig. 7. Development of dimensionless axial velocity w along y at the symmetry plane for $Ra_q = 9.35 \times 10^5$, $Pr = 37.1$ and $Q = 5.0$ with only upper wall heated.

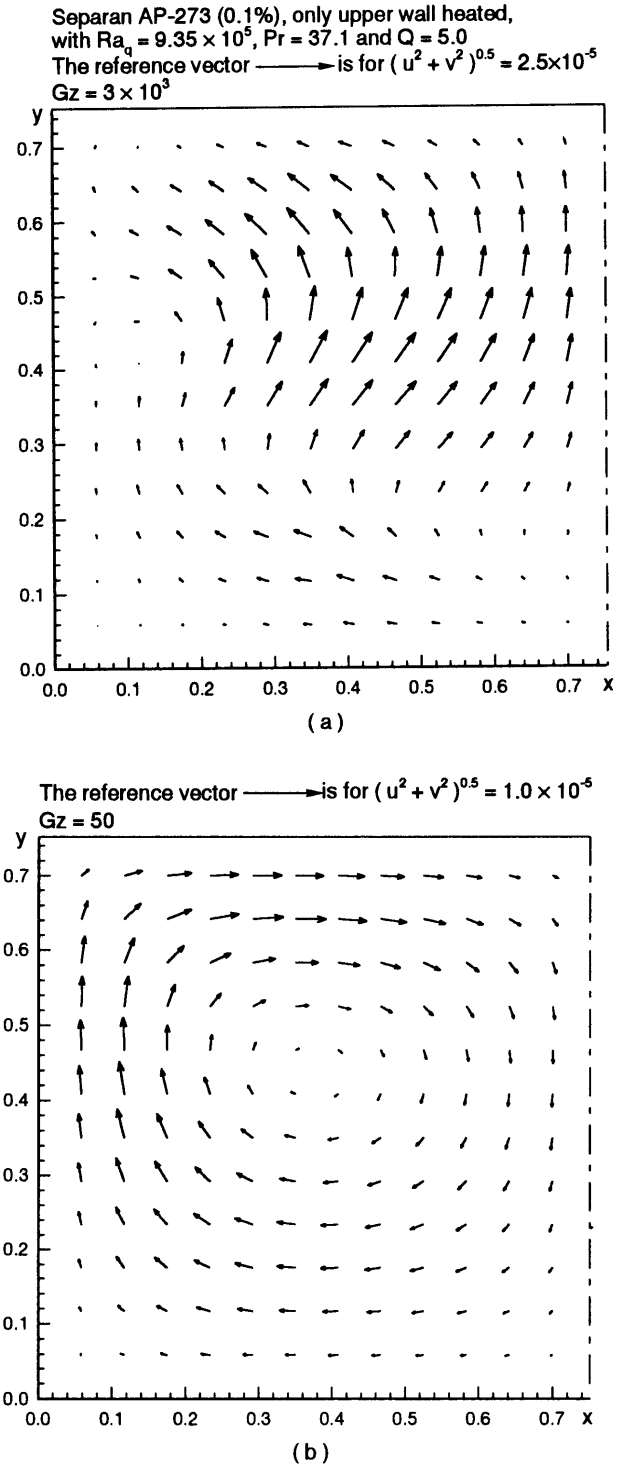

Fig. 8. Development of secondary flow for $Ra_q = 9.35 \times 10^5$, $Pr = 37.1$ and $Q = 5.0$ with only upper wall heated.

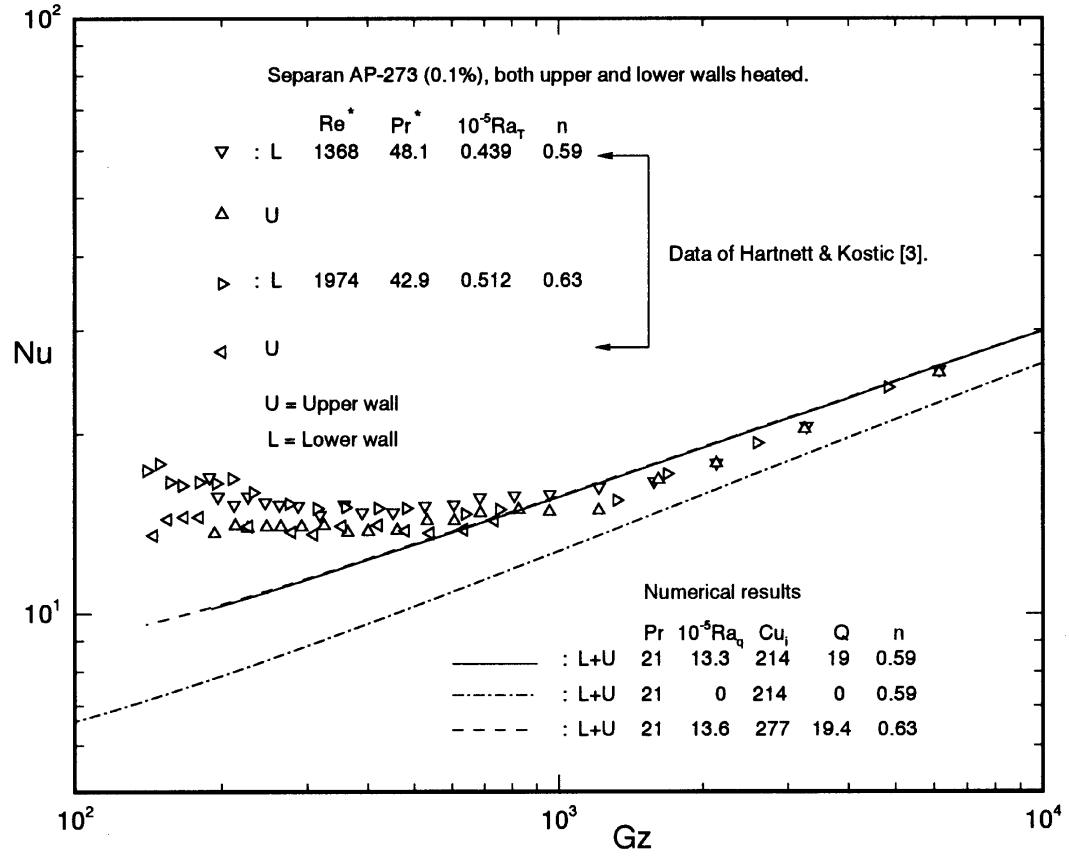

Fig. 9. The comparison of the present numerical results of *Nu* with experimental data for Separan solution under the heating condition of both upper and lower walls heated.

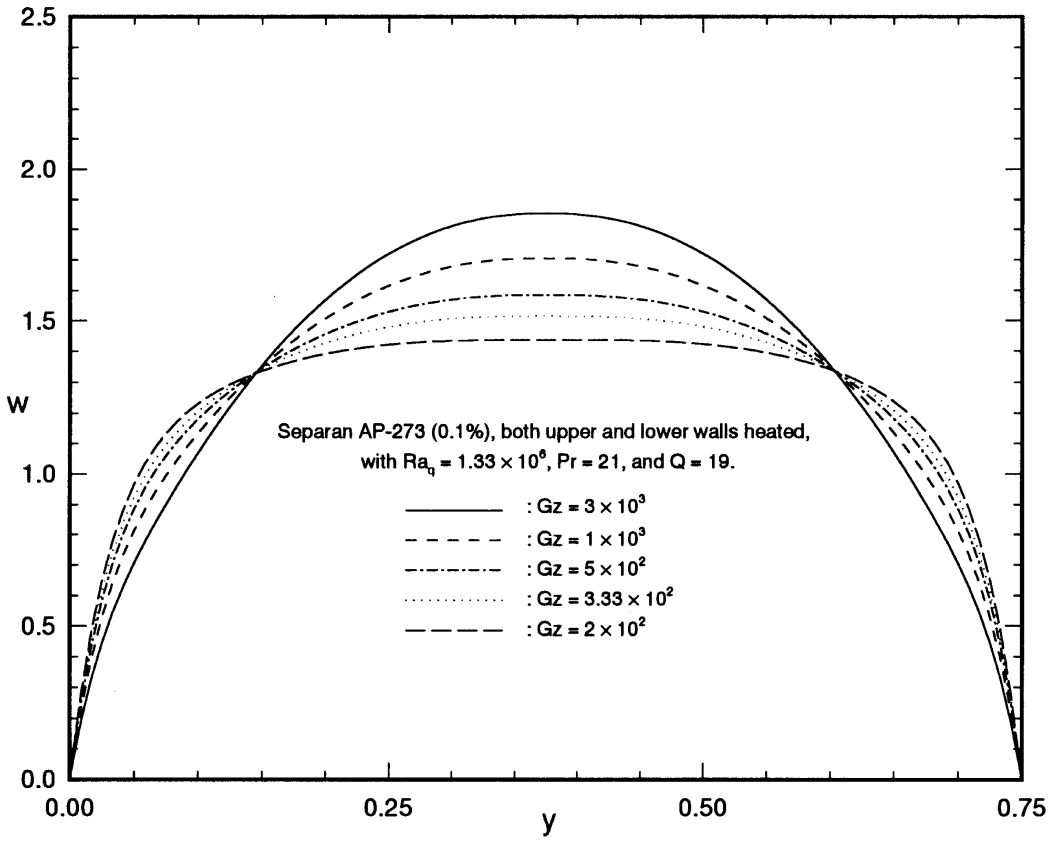

Fig. 10. Development of dimensionless axial velocity w along y at the symmetry plane for $Ra_q = 1.33 \times 10^6$, $Pr = 21$ and $Q = 19$ with both upper and lower walls heated.

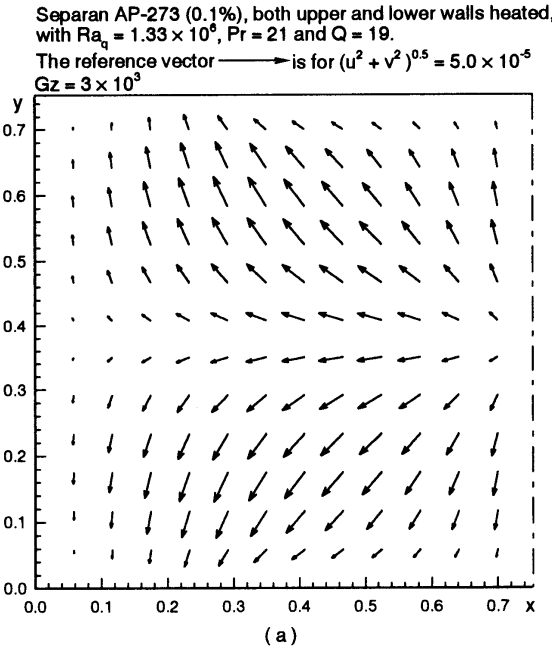

Fig. 11. Development of secondary flow for $Ra_q = 1.33 \times 10^6$, $Pr = 21$ and $Q = 19$ with both upper and lower walls heated.

an asymptotic value for the case of only upper wall heated. While for the case of both upper and lower walls heated, Nusselt number decreases at first, and then gradually increases due to the effect of buoyancy-induced secondary flow.

(2) For non-Newtonian fluid, Separan solution, the effects of temperature dependence and shear thinning on viscosity significantly influence the heat transfer mechanism especially in the region near the entrance. And the heat transfer enhancement is caused mainly by the axial velocity distortion.

(3) By the inspection of the developments of axial velocity distributions, one can find that the velocity distributions are more and more distorted toward the heated upper wall for the case of only upper wall heated. While for the case of both upper and lower walls heated, the velocity distributions are more and more flat, the velocity distributions are symmetrically distorted toward the heated upper and lower walls.

(4) The effect of buoyancy-induced secondary flow are much weaker in the case for Separan solution than that shown in the case for water. It is mainly caused by that the value of Rayleigh number is rather low if we evaluate it by the viscosity of fluid around the central zone of rectangular duct. At the central zone of duct, the temperature and shear rate of fluid are all relatively lower, and then the viscosity is relatively higher than that near the walls.

Acknowledgement

Financial support from the National Science Council of Republic of China through Project NSC 85-2212-E008-009 is greatly appreciated.

References

[1] Hartnett JP. Viscoelastic fluids: a new challenge in heat transfer. J Heat Transfer 1992;114:296–303.
[2] Xie C, Hartnett JP. Influence of rheology on laminar heat transfer to viscoelastic fluids in a rectangular channel. Ind Eng Chem Res 1992;31:727–32.
[3] Hartnett JP, Kostic M. Heat transfer to a viscoelastic fluid in laminar flow through a rectangular channel. Int J Heat Mass Transfer 1985;28:1147–55.
[4] Sieder EN, Tate GE. Heat transfer and pressure drop of liquids in tubes. Ind Engng Chem 1936;23:1429–35.
[5] Deissler RG. Analytical investigation of fully developed laminar flow in tubes with heat transfer with fluid properties variable along the radius. NACA TN 2410, Washington, July 1951.
[6] Yang KT. Laminar forced convection of liquids in tubes with variable viscosity. J Heat Transfer 1962;84:353–62.
[7] Test FL. Laminar flow heat transfer and fluid flow for liquids with temperature-dependent viscosity. J Heat Transfer 1968;90:385–93.
[8] Shannon RL, Depew CA. Forced laminar flow convection

in a horizontal tube with variable viscosity and free convection effects. J Heat Transfer 1969;91:251–8.
[9] Hong S, Bergles AE. Theoretical solutions for combined forced and free convection in horizontal tubes with temperature-dependent viscosity. J Heat Transfer 1976;98:459–65.
[10] Butler HW, Mckee DE. An exact solution for the flow of temperature-dependent viscous fluids in heated rectangular ducts. J Heat Transfer 1973;95:555–7.
[11] Kostic M. On turbulent drag and heat transfer reduction phenomena and laminar heat transfer enhancement in non-circular duct flow of certain non-Newtonian fluids. Int J Heat Mass Transfer 1994;37 Suppl 1:133–47.
[12] Xie C, Hartnett JP. Influence of variable viscosity of mineral oil on laminar heat transfer in a 2 : 1 rectangular duct. Int J Heat Mass Transfer 1992;35:641–8.
[13] Shin S, Cho YI, Gingrich WK, Shyy W. Numerical study of laminar heat transfer with temperature dependent fluid viscosity in a 2 : 1 rectangular duct. Int J Heat Mass Transfer 1993;36:4365–73.
[14] Chou FC, Tung CW. The mechanism of heat transfer enhancement for mineral oil in 2 : 1 rectangular ducts. Int J Heat Mass Transfer 1995;38:2863–71.
[15] Gingrich WK, Cho YI, Shyy W. Effects of shear thinning on laminar heat transfer behavior in a rectangular duct. Int J Heat Mass Transfer 1992;35:2823–36.
[16] Shin S, Cho YI. Temperature effect on the non-Newtonian viscosity of an aqueous polyacrylamide solution. Int Comm Heat Mass Transfer 1993;20:831–44.
[17] Gervang B, Larsen PS. Secondary flows in straight ducts of rectangular cross section. J Non-Newtonian Fluid Mechanics 1991;39:217–37.
[18] Gao SX, Hartnett JP. Non-Newtonian laminar flow and forced convection heat transfer in rectangular ducts. Int Commun Heat Mass Transfer 1992;19:673–86.
[19] Shin S, Cho YI. Laminar heat transfer in a rectangular duct with a non-Newtonian fluid with temperature-dependent viscosity. Int J Heat Mass Transfer 1994;37:19–30.
[20] Gao SX, Hartnett JP. Steady flow of non-Newtonian fluids through rectangular ducts. Int Commun Heat Mass Transfer 1993;20:197–210.
[21] Gao SX, Hartnett JP. Heat transfer behavior of Reiner–Rivlin fluids in rectangular ducts. Int J Heat Mass Transfer 1996;39:1317–24.
[22] Kwant PB, Van Ravenstein TNM. Non-isothermal laminar channel flow. Chem Eng Sci 1973;28:1935–50.
[23] Chou FC, Tsou FK, Tung CW. Numerical studies of non-Newtonian channel flow and heat transfer enhancement for electronics modules. ASME J Electronic Packaging 1995;117:246–9.
[24] Bird RB, Armstrong RC, Hassager O. Dynamics of polymeric liquids. New York : John Wiley, 1987.
[25] Chou FC, Hwang GJ. Vorticity–velocity method for the Graetz problem and the effect of natural convection in a horizontal rectangular channel with uniform wall heat flux. J Heat Transfer 1987;109:704–10.
[26] Kostic M. Heat transfer and hydrodynamics of water and viscoelastic fluid flow in a rectangular duct. Ph.D. dissertation, Mechanical Engineering Department, University of Illinois at Chicago, 1984.
[27] Xie C. Laminar heat transfer of Newtonian and non-Newtonian fluids in a 2 : 1 rectangular duct. Ph.D. dissertation, Mechanical Engineering Department, University of Illinois at Chicago, 1991.